Yttrium iron garnet thickness and frequency dependence of the spin-charge current conversion in YIG/Pt systems

V. Castel, N. Vlietstra,* and B. J. van Wees
Physics of Nanodevices, Zernike Institute for Advanced Materials, University of Groningen, Groningen, The Netherlands

J. Ben Youssef
Laboratoire de Magnétisme de Bretagne, CNRS, Université de Bretagne Occidentale, Brest, France
(Received 8 April 2013; revised manuscript received 4 December 2014; published 22 December 2014)

We report the frequency dependence of the spin current emission (spin pumping) in a hybrid ferrimagnetic insulator/normal metal system as a function of the insulating layer thickness. The system is based on an yttrium iron garnet (YIG) film [0.2, 1, and 3 μm] grown by liquid-phase epitaxy coupled with a spin current detector of platinum[6 nm]. A strong YIG thickness dependence of the efficiency of the spin pumping has been observed. The highest conversion factor $\Delta V/P_{\text{abs}}$ has been demonstrated for the thinner YIG (1.79 and 0.55 mV/mW at 2.5 and 10 GHz, respectively), which is of interest for research heading towards YIG-based devices. Furthermore, we demonstrate the threshold frequency dependence of the three-magnon splitting process, which is shown to cease to exist for the thinner YIG of 0.2 μm.

DOI: 10.1103/PhysRevB.90.214434 PACS number(s): 72.25.Pn, 72.15.−v, 75.78.−n, 75.30.Ds

Recently in the field of spintronics, Kajiwara *et al.* [1] opened a renewed interest by the demonstration of the spin pumping and inverse spin Hall effect (ISHE) processes in a hybrid system based on yttrium iron garnet (YIG) coupled with a layer of platinum (Pt). The YIG/Pt system presents an important role for future electronic devices based on nonlinear dynamics effects [2–6]. One such nonlinear effect is the three-magnon splitting process. This process can influence the conversion efficiency of a spin current from spin pumping as a function of both the frequency (or magnetic field) and the YIG thickness [7,8].

In this paper, we show the experimental observation of the YIG thickness dependence of the dc voltage generation from spin pumping in a hybrid YIG/Pt system, actuated at the resonant condition over a large frequency range [9,10]. We demonstrate that the three-magnon splitting process ceases to exist for the thinner YIG of 0.2 μm, which is much smaller than the exchange interaction length in such a system [8].

The used insulating material consists of a single-crystal (111) $Y_3Fe_5O_{12}$ (YIG) film grown on a (111) $Gd_3Ga_5O_{12}$ (GGG) substrate by liquid-phase epitaxy. Three samples with different thicknesses of YIG [0.2, 1, and 3 μm] have been investigated. For each sample a 6-nm-thick Pt layer grown by dc sputtering has been used as a spin current detector [11]. Several steps of electron beam lithography have been performed in order to pattern the Pt area (600 × 30 μm), the stripe antenna, the insulating layer of Al_2O_3 between them, and the electrical contacts. Both the stripe antenna (60 μm width) and the electrodes for the electrical contacts consist of a layer of Ti/Au. A signal-ground picoprobe has been used in order to connect the antenna to the network analyzer. A schematic of the sample including the microstripe antenna is shown in the inset of Fig. 1(b).

The used device configuration allows us to simultaneously detect the dc voltage generation in the Pt layer (V_{ISHE}) and of the ferromagnetic response (microwave absorption) of the system, as is shown in Figs. 1(a) and 1(b), respectively (without modulation and lock-in detection) [12]. In these figures, ΔV and ΔS_{11} correspond to the magnitude of V_{ISHE} and to the microwave absorption power at the resonant condition f_{FMR}, respectively. S_{11} corresponds to the reflection coefficient extracted from the scattering parameter of the network analyzer (in one port configuration). The microwave absorption in Fig. 1(b) corresponds to the difference between the S_{11} spectrum for the resonance in the YIG layer and from a spectrum taken at a nonresonant field. An example is presented in Fig. 2 for a static magnetic field of 3 kOe. The magnitude of the baseline for all used samples and for different values of the static magnetic field is equal to 0 dBm (1 mW).

A nonzero V_{ISHE} comes from the fact that at (and close to) f_{FMR} a spin current (j_s) is pumped into the Pt layer, which results in a dc voltage by the ISHE. In this system, the pumped spin current originates from the spin exchange interaction at the interface between localized moments in the YIG and conduction electrons in the Pt layer. The static magnetic field (H) used to define the magnetization direction of the YIG is applied in the plane of the device and oriented perpendicularly to the length of the Pt layer [along x; see inset Fig. 1(b)], such that the ISHE signal is maximized [13]. One can see in Fig. 1(b) that the FMR line is asymmetric and has a broader tail for $f > f_{\text{FMR}}$, mainly due to the contribution of the magnetostatic surface spin waves (MSSWs) [14,15].

Similar measurements to those presented in Fig. 1 have been performed for the different thicknesses of YIG. For each sample, the dc voltage generation (V_{ISHE}) and the ferromagnetic response (S_{11}) have been studied as a function of frequency and applied magnetic field at an rf power of 10 mW. Figures 3(a) and 3(b) give a summary of the frequency dependence of the microwave absorption P_{abs} and the dc voltage ΔV, respectively. For converting the measured microwave absorption in dBm to the absorbed power in mW the equation $P_{\text{abs}}[\text{mW}] \propto 10^{|S_{11}^{\text{FMR}}|/10} - 1$ has been used.

By increasing the thickness of the YIG layer, the magnitude of the absorbed power is enhanced. This is due to the fact

*Corresponding author: n.vlietstra@rug.nl

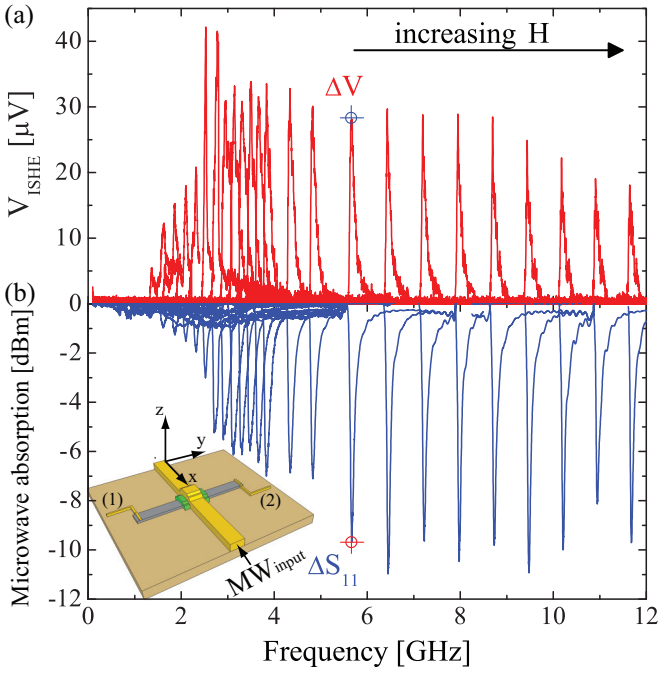

FIG. 1. (Color online) Frequency dependence of (a) the dc voltage from spin pumping (V_{ISHE}), and (b) the microwave absorption determined by the scattering parameter S_{11}, for different values of the static magnetic field (H) applied in the plane of the substrate along the x direction. The thickness of the YIG layer is 1 μm. For each value of H, the excitation frequency has been swept at an rf power of 10 mW (at room temperature). ΔV and ΔS_{11} correspond to the magnitude of V_{ISHE} and S_{11} at the resonant condition, respectively. The inset represents the measurement configuration. (1) and (2) are the electrical contacts, the gray area corresponds to the Pt layer, the green is the Al_2O_3 layer, the yellow stripe is the microwave antenna, and the brown part shows the YIG.

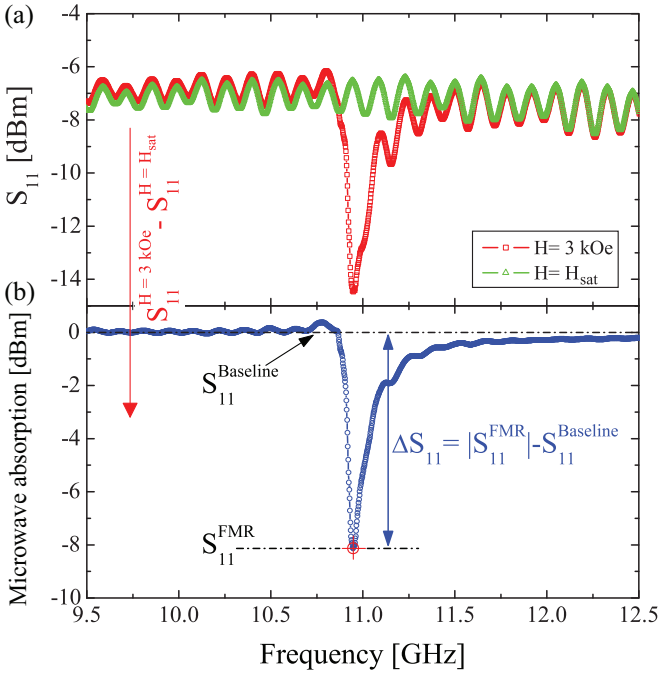

FIG. 2. (Color online) (a) Frequency dependence of the S_{11} spectrum measured at $H = 3$ kOe (in red) and at a saturation field H_{sat} (in green) equal to 4 kOe for a YIG thickness of 1 μm. The measurement has been performed at an rf power of 10 mW at room temperature. (b) Frequency dependence of the microwave absorption corresponding to the difference between the S_{11} spectrum for the resonance in the YIG layer ($H = 3$ kOe) and from the spectrum without resonance signature (H_{sat}). $S_{11}^{\mathrm{Baseline}}$ and S_{11}^{FMR} correspond to the magnitude of the microwave absorption in dBm, of the baseline and at the resonant condition, respectively.

that P_{abs} is a function of the volume of YIG (v), interacting with the microwave field (h_{rf}) following the equation $P_{\mathrm{abs}} = \pi\mu_0 v f_{\mathrm{FMR}} \chi^{\parallel} h_{\mathrm{rf}}^2$. Here, μ_0 and $\chi^{\parallel}$ are the permeability in vacuum and the imaginary part of the magnetic dynamic susceptibility, respectively. Note that the absorbed power is not enhanced much for the 3 μm sample compared to the 1 μm sample. This is a result of absorption saturation caused by the maximum available rf power of 10 mW.

The general trend of P_{abs} as function of the frequency is almost the same for the different thicknesses of YIG and presents two regimes: For frequencies lower than 3.3 GHz, the absorbed power is reduced by decreasing the frequency. For frequencies higher than 3.3 GHz, P_{abs} presents a nearly constant value around 0.4 and 10.0 mW for a thickness of 0.2 and 1 (also 3) μm, respectively.

The YIG thickness dependence of the magnitude of ΔV, as is shown in Fig. 3(b), does not present the same dependence as for P_{abs}. Where P_{abs} decreases, an increase of ΔV is observed as a function of decreasing YIG thickness. For example around 9 GHz, ΔV reaches 247, 28.5, and 14.5 μV at 10 mW for a YIG thickness of 0.2, 1, and 3 μm, respectively. Furthermore, for a given YIG thickness, ΔV increases in the frequency range of 1 to 2.4–2.8 GHz and up to 4 GHz the magnitude of ΔV is nearly constant. Note that the decrease of ΔV from the maximum to the constant value is abrupt for the 1 and 3 μm YIG layers, which is not the case for the thinner 0.2 μm YIG layer. Additionally, ΔV obtained for the 0.2 μm YIG layer is one order of magnitude larger than the value of ΔV for both thicker YIG layers.

In order to understand the frequency dependence of the spin current generation for the different thicknesses of YIG and to confirm the existence of the abrupt change of ΔV, demonstrated in Fig. 3(b), we have calculated the factor $\Delta V/P_{\mathrm{abs}}$ introduced by Kurebayashi *et al.* [3] (see also Ref. [16]) as is shown in Fig. 4. The factor $\Delta V/P_{\mathrm{abs}}$ corresponds to the conversion efficiency of the angular momentum created by the microwave field into the spin current and it is described by the following equation, extracted from Ref. [3]:

$$\frac{\Delta V}{P_{\mathrm{abs}}} = A \frac{1}{\sqrt{1 + \left(\frac{4\pi f}{\gamma M_S}\right)^2}}, \tag{1a}$$

$$A = \frac{eL\Theta_{SH} g_{\uparrow\downarrow} \lambda \tanh(t_{\mathrm{Pt}}/2\lambda)}{\pi\mu_0 \nu t_{\mathrm{Pt}} \sigma M_S^2 \alpha}, \tag{1b}$$

where e is the elementary charge. L, t_{Pt}, λ, σ are the distance between the electrodes, the thickness of the Pt layer, the spin diffusion length, and the electric conductivity, respectively. Θ_{SH} and $g_{\uparrow\downarrow}$ are the spin-Hall angle and the spin-mixing conductance, respectively. Characteristics of the YIG layer are

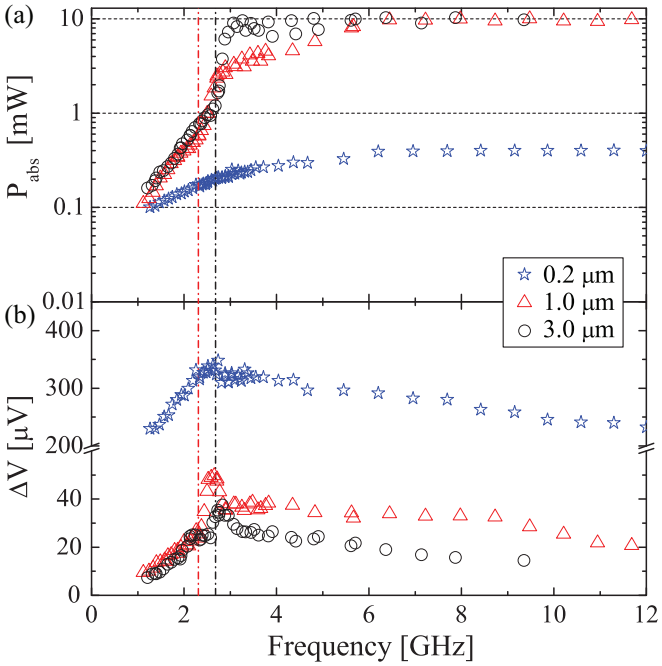

FIG. 3. (Color online) Frequency dependence of (a) the microwave absorption ΔS_{11} in mW and (b) the dc voltage ΔV, for different thicknesses of YIG [0.2, 1, and 3 μm]. Vertical dashed-dotted lines correspond to the frequency cutoff of the three-magnon splitting process estimated using the dispersion relation of spin waves for a YIG thickness of 1 (red) and 3 μm (black). All measurements have been carried out at room temperature under an rf excitation of 10 mW.

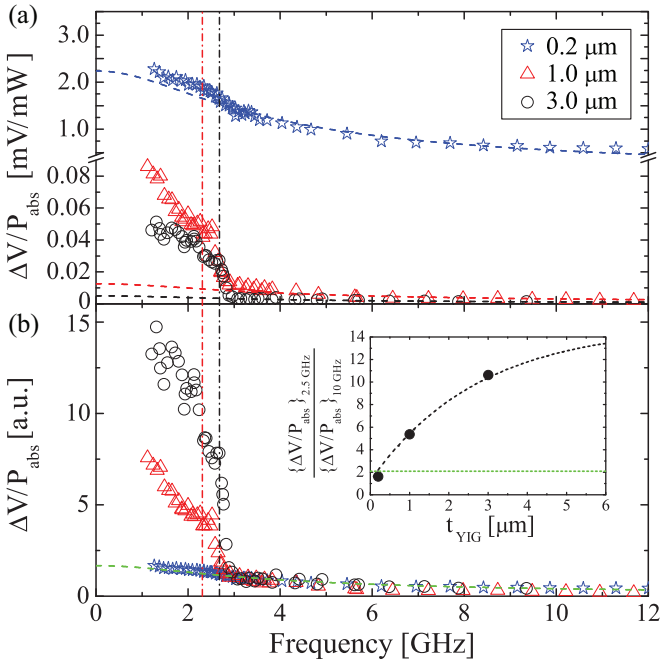

FIG. 4. (Color online) (a) Frequency dependence of the conversion efficiency factor $\Delta V/P_{abs}$ for different thicknesses of YIG [0.2, 1, and 3 μm]. (b) $\Delta V/P_{abs}$ normalized by its value at 3.3 GHz. The vertical dashed-dotted lines correspond to the frequency cutoff of the three-magnon splitting process, for a YIG thickness of 1 (red) and 3 μm (black). The green, blue, red, and black dashed curves correspond to the theoretical frequency dependence of $\Delta V/P_{abs}$ from Eq. (1). The inset in (b) shows the dependence of the ratio of $\Delta V/P_{abs}$ at 2.5 and 10 GHz as a function of the thickness of the YIG layer. The green dashed line shows the theoretical expected magnitude of this ratio and the black dashed line is a guide to the eye.

defined by the saturation magnetization M_S, the gyromagnetic ratio γ, and the Gilbert damping parameter α. ν is the excited volume of the YIG at a frequency f and introduces the YIG thickness dependence of $\Delta V/P_{abs}$.

The frequency dependence of Eq. (1) is introduced by the expression of the spin current (j_s) [17,18] and the magnetic susceptibility, which can be written as

$$\frac{\Delta V}{P_{abs}} \propto \frac{j_s}{f\chi_{\parallel} h_{rf}^2} \propto \int_0^{1/f} \frac{1}{\chi_{\parallel} h_{rf}^2} \left\langle M(t) \times \frac{dM(t)}{dt} \right\rangle_z dt. \quad (2)$$

By solving the Landau-Lifshiftz-Gilbert equation for the FMR condition of the integral in Eq. (2), the right part of Eq. (1a) is calculated (see supplementary information in Ref. [3]).

In Fig. 4(a) one can see that for frequencies higher than 3.3 GHz, the experimental frequency dependence of $\Delta V/P_{abs}$ follows the theoretical behavior calculated from Eq. (1) (shown by de dashed lines). In the low-frequency range (lower than 3.3 GHz), the evolution of the conversion factor $\Delta V/P_{abs}$ is different for the thinner [0.2 μm] compared to the thicker YIG [1 and 3 μm] and several points should be made regarding this evolution. First, for thicker YIG [1 and 3 μm], one can observe the same signature of the enhancement of $\Delta V/P_{abs}$ in the low-frequency range [1–3.3 GHz], as demonstrated by Kurebayashi *et al.* [3] for a YIG thickness of 5.1 μm. Nevertheless, for the thinner YIG of 0.2 μm, no enhancement of $\Delta V/P_{abs}$ with respect to the theoretical behavior (dashed lines in Fig. 4) has been observed.

The good agreement between experiments and the theoretical description given by Eq. (1) in the frequency range [3.3–12 GHz] confirms the fact that in this range V_{ISHE} is directly proportional to the spin current generated by the magnetization precession of the uniform mode (long wavelength). However, V_{ISHE} is insensitive to the spin-wave wavelength, so the measured ΔV can also be generated by other spin-wave modes, for example short-wavelength modes. Such modes might explain the observed enhancement of ΔV in the low-frequency range [3,6].

In Fig. 4(b), $\Delta V/P_{abs}$ has been normalized by the values of this quantity at $f = 3.3$ GHz for the different YIG-thicknesses. At low frequency, the normalized conversion efficiency is enhanced by increasing the YIG thickness. This observation is well represented in the inset of Fig. 4(b), which shows the evolution of the ratio of $\Delta V/P_{abs}$ at 2.5 and 10 GHz as a function of the YIG thickness. The enhancement of the YIG thickness from 1 to 3 μm induces an increase of this ratio from 5 to 11. For the thinner YIG, this ratio is equal to 2 and corresponds to the theoretical value represented by the horizontal green dashed line.

The enhancement of $\Delta V/P_{abs}$ at low frequencies for thicker YIG layers can be explained by the three-magnon splitting process. The possibility to control the spin current at the YIG/Pt interface by the three-magnon splitting process has

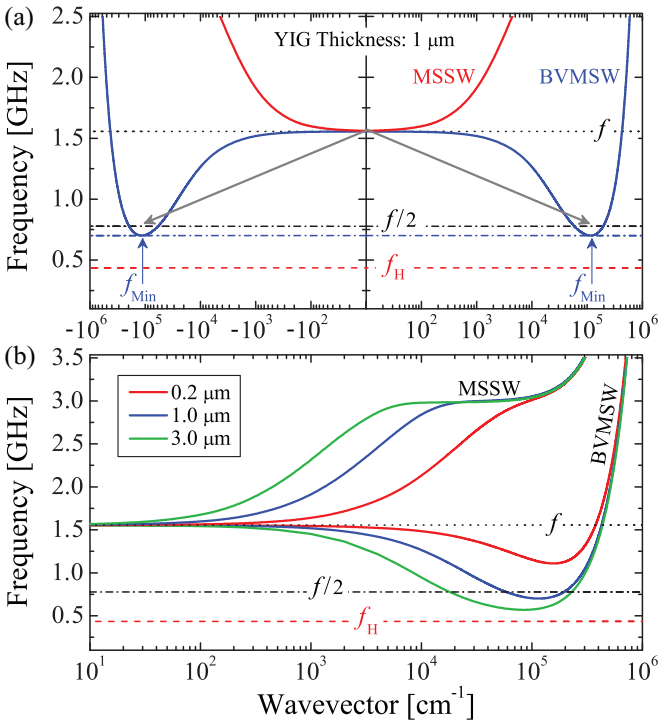

FIG. 5. (Color online) Dispersion relation of spin waves [19,20]. (a) Dependence of the frequency f, as a function of the wave vector k, when $k \parallel H$ (BVMSW) and $k \perp H$ (MSSW) for a YIG thickness of 1 μm. The arrows represent the three-magnon splitting process that creates two spin waves with a frequency corresponding to $f/2$. $f_{\min}$ gives the minimum possible frequency of the BVMSW modes. (b) Evolution of the spin-wave spectrum for different thicknesses of YIG [0.2, 1, and 3 μm]. For increasing YIG thickness, it shows that $f_{\min}$ decreases, and finally approaches the Larmor frequency f_H. In both figures, the magnetic field is fixed at 150 Oe ($f = f_{\mathrm{FMR}} = 1.55$ GHz). The exchange stiffness has been fixed at $D = 2 \times 10^{-13}$ Oe^{-1} m^2 (see Ref. [21]).

been demonstrated by Kurebayashi *et al.* [3]. This process is a nonlinear effect easily actuated at low rf power (on the order of a few μW) due to the low damping parameter of YIG, which is two orders of magnitude smaller than that of Permalloy ($Ni_{19}Fe_{81}$).

Figure 5(a) presents the dependence of the frequency (f), as a function of the wave vector (k), for both $k \parallel H$ (backward volume magnetostatic spin wave, BVMSW) and $k \perp H$ (MSSW), estimated from the dispersion relation of spin waves from Refs. [19,20]. The arrows represent the three-magnon splitting process that creates two spin waves (short wavelength with $k \sim 10^5$ cm^{-1}) from the uniform mode (long wavelength with $k \sim 0$ cm^{-1}). The created magnons have a frequency corresponding to half of the excitation frequency ($f/2$). The minimum of the BVMSW dispersion curve corresponds to the minimum possible spin-wave frequency ($f_{\min}$), which results from the competition between the magnetic field dipole interaction and the exchange interaction [20,22]. A simple rule for the frequency range selection of the existence of the three-magnon splitting process can be deduced from this graph: The three-magnon splitting process is only allowed if $f/2 > f_{\min}$, which means that this nonlinear effect presents a frequency cutoff, f_{cutoff}.

Figure 5(b) shows the evolution of the spin-wave spectrum for different thicknesses of YIG [0.2, 1, and 3 μm], calculated by fixing the magnetic field at 150 Oe ($f = f_{\mathrm{FMR}} = 1.55$ GHz). $f_{\min}$ depends of the thickness of the YIG layer which induces an evolution of f_{cutoff} until a critical thickness where the three-magnon splitting process is no longer allowed [7,8]. When the thickness of the YIG increases, $f_{\min}$ approaches the Larmor frequency f_{H}. In this particular case, $f_{\mathrm{cutoff}} = \frac{2}{3}\gamma\mu_0 M_S$ which is around 3.3 GHz for typical values of γ and M_S.

For each YIG thickness, $f_{\min}$ has been calculated for different values of the magnetic field and a fixed exchange stiffness $D = 2 \times 10^{-13}$ Oe^{-1} m^2 (see Ref. [21]) using the dispersion relation of spin waves [19,20]. For the YIG thickness of 0.2 μm, the three-magnon splitting condition $f/2 > f_{\min}$ is never reached, for the whole frequency range; showing that this process ceases to exist for this YIG thickness. The absence of the three-magnon splitting is proven by Fig. 4, where no sudden enhancement of $\Delta V/P_{\mathrm{abs}}$ is observed for the 0.2 μm sample. The theoretical values of f_{cutoff} for the YIG thicknesses of 1 and 3 μm (2.35 and 2.7 GHz, respectively) are represented by the vertical dashed-dotted lines in Figs. 3 and 4 and are in good agreement with the experiment's thresholds.

Despite the fact that the three-magnon splitting process is not allowed for the thinner YIG, the conversion efficiency of this sample as presented in Fig. 4(a) is huge compared to the thicker YIG layers. To understand this enhancement, we have a closer look to the factor A in Eq. (1). This factor is defined by a product of fundamental constants (e,π,μ_0), geometrical and materials parameters of YIG (ν,α,γ,M_S), of Pt (L,t_{Pt},λ,σ,Θ_{SH}), and of the interface ($g_{\uparrow\downarrow}$). Tashiro *et al.* [23] have demonstrated experimentally that $g_{\uparrow\downarrow}$ is independent of the YIG thickness, which is consistent with the fact that the spin pumping (in the linear regime) is defined by the exchange interaction at the YIG/Pt interface. The saturation magnetization has been measured by a vibrating sample magnetometer and indicated that this parameter is also independent of the YIG thickness (1760 G). γ has been extracted from the fitting of the experimental magnetic field dependence of the resonant frequency (f_{FMR}), by using the Kittel equation [24]. It presents almost the same value for the different thicknesses of YIG, between 1.81 and 1.82 $\times 10^7$ rad Oe^{-1} s^{-1}. In addition, parameters of the Pt layer are the same for the measured set of samples as the different deposition steps (Pt, Ti/Au, and Al_2O_3) have been done simultaneously for all samples. Therefore, the only parameters in A which can explain the observed large conversion efficiency for the thinner YIG are the YIG thickness (via ν) and the damping parameter α.

The contribution of α can be investigated by comparing the linewidth ΔF_{FMR} of the different FMR spectra. Due to the fact that several modes contribute to the spin pumping (volume and surface), the FMR and the V_{ISHE} lines in Fig. 1 are broadened. In this case, one can only estimate the linewidth ΔF of the full spectrum. In the high-frequency range (>4 GHz) we find $\Delta F = 50$, 85, and 135 MHz for the YIG thickness of 0.2, 1, and 3 μm, respectively. The linewidth

determined in this way does not necessarily match with the intrinsic FMR linewidth, ΔF_{FMR}, of the uniform mode, but is proportional to it ($\alpha \propto \Delta F_{\mathrm{FMR}} \propto \Delta F$). By normalizing the factor A [determined using the fits shown in Fig. 4(a)] with the YIG thickness and the measured ΔF (proportional to α), we observe a factor 12 to 20 enhancement of A for the thinner YIG of 0.2 μm ($A_{\mathrm{norm}} = 2.3 \times 10^{-2}$) as compared to the thicker YIG samples of 1 and 3 μm ($A_{\mathrm{norm}} = 1.2 \times 10^{-3}$ and $A_{\mathrm{norm}} = 2.0 \times 10^{-3}$, respectively). This is not in agreement with the expected constant value of A after the normalization.

There are many phenomena which can induce the creation of spin waves with short wavelength. At first, the enhancement of A might be explained by the so-called two-magnon process. This effect occurs due to the scattering of magnons on impurities and surfaces of the film and can contribute to the enhancement of the spin current at the YIG/Pt interface [6]. Second, it is well known that the distribution of precession amplitude of the MSSWs across the film thickness is exponential, with its maximum at the surface of the film [25]. Contrary, the BVMSWs are characterized by a harmonic distribution of the dynamic magnetization across the film thickness, and its magnitude is thus small at the surface of the film. So, as the dynamic magnetization of the MSSWs is localized at the surface, the contribution of these waves to the dc voltage from spin pumping will be higher than the contribution of the BVMSWs [15]. It might be possible that the contribution of these different types of waves to the dc voltage generation is changed for thin YIG due to the fact that a reduction of the YIG thickness induces an enhancement (reduction) of the delay times (group velocity) of the spin waves.

In summary, we have reported the frequency dependence of the spin current emission in a hybrid YIG/Pt [6 nm] system as function of the YIG thickness [0.2, 1, and 3 μm], actuated at the resonant condition over a large frequency range [1–12 GHz]. We have demonstrated the possibility to control the efficiency of the spin current conversion by changing the YIG thickness and we have observed the frequency- and YIG-thickness-dependence of the three-magnon splitting process. We have experimentally brought the evidence of the nonexistence of this nonlinear effect for a thin layer of YIG [0.2 μm]. Additionally, we observe a huge conversion factor $\Delta V/P_{\mathrm{abs}}$ for the thinner YIG (1.79 and 0.55 mV/mW at 2.5 and 10 GHz, respectively), which originates from another phenomenon present in the YIG. This high conversion factor is an interesting feature, which might be used for the realization of YIG-based devices.

We would like to acknowledge B. Wolfs, M. de Roosz, and J. G. Holstein for technical assistance. This work is part of the research program (Magnetic Insulator Spintronics) of the Foundation for Fundamental Research on Matter (FOM) and is supported by NanoNextNL, a micro- and nanotechnology consortium of the Government of the Netherlands and 130 partners, by NanoLab NL, and the Zernike Institute for Advanced Materials.

[1] Y. Kajiwara, K. Harii, S. Takahashi, J. Ohe, K. Uchida, M. Mizuguchi, H. Umezawa, H. Kawai, K. Ando, K. Takanashi, S. Maekawa, and E. Saitoh, Nature (London) **464**, 262 (2010).
[2] K. Ando and E. Saitoh, Phys. Rev. Lett. **109**, 026602 (2012).
[3] H. Kurebayashi, O. Dzyapko, V. E. Demidov, D. Fang, A. J. Ferguson, and S. O. Demokritov, Nat. Mater. **10**, 660 (2011).
[4] C. W. Sandweg, Y. Kajiwara, A. V. Chumak, A. A. Serga, V. I. Vasyuchka, M. B. Jungfleisch, E. Saitoh, and B. Hillebrands, Phys. Rev. Lett. **106**, 216601 (2011).
[5] H. Kurebayashi, O. Dzyapko, V. E. Demidov, D. Fang, A. J. Ferguson, and S. O. Demokritov, Appl. Phys. Lett. **99**, 162502 (2011).
[6] M. B. Jungfleisch, A. V. Chumak, V. I. Vasyuchka, A. A. Serga, B. Obry, H. Schultheiss, P. A. Beck, A. D. Karenowska, E. Saitoh, and B. Hillebrands, Appl. Phys. Lett. **99**, 182512 (2011).
[7] V. Castel, N. Vlietstra, B. J. van Wees, and J. Ben Youssef, Phys. Rev. B **86**, 134419 (2012).
[8] A. L. Chernyshev, Phys. Rev. B **86**, 060401 (2012).
[9] Recently a paper by Dzyapko *et al.* [10] was published, showing similar experiments.
[10] O. Dzyapko, H. Kurebayashi, V. E. Demidov, M. Evelt, A. J. Ferguson, and S. O. Demokritov, Appl. Phys. Lett. **102**, 252409 (2013).
[11] V. Castel, N. Vlietstra, J. Ben Youssef, and B. J. van Wees, Appl. Phys. Lett. **101**, 132414 (2012).
[12] Contrary to the experiments described in Refs. [7,11], for the work shown here, simultaneous detection of the dc voltage and the ferromagnetic response was possible, due to the improved sample geometry (on-chip antenna).
[13] E. Saitoh, M. Ueda, H. Miyajima, and G. Tatara, Appl. Phys. Lett. **88**, 182509 (2006).
[14] D. D. Stancil and A. Prabhakar, *Spin Waves: Theory and Applications* (Springer, New York, 2009).
[15] C. W. Sandweg, Y. Kajiwara, K. Ando, E. Saitoh, and B. Hillebrands, Appl. Phys. Lett. **97**, 252504 (2010).
[16] K. Harii, T. An, Y. Kajiwara, K. Ando, H. Nakayama, T. Yoshino, and E. Saitoh, J. Appl. Phys. **109**, 116105 (2011).
[17] Y. Tserkovnyak, A. Brataas, and G. E. W. Bauer, Phys. Rev. Lett. **88**, 117601 (2002).
[18] Y. Tserkovnyak, A. Brataas, and G. E. W. Bauer, Phys. Rev. B **67**, 140404 (2003).
[19] B. A. Kalinikos, M. P. Kostylev, N. V. Kozhus, and A. N. Slavin, J. Phys.: Condens. Matter **2**, 9861 (1990).
[20] B. A. Kalinikos and A. N. Slavin, J. Phys. C: Solid State Phys. **19**, 7013 (1986).
[21] S. M. Rezende, Phys. Rev. B **79**, 174411 (2009).
[22] A. Kreisel, F. Sauli, L. Bartosch, and P. Kopietz, Eur. Phys. J. B **71**, 59 (2009).
[23] T. Tashiro, R. Takahashi, Y. Kajiwara, K. Ando, H. Nakayama, T. Yoshino, D. Kikuchi, and E. Saitoh, Proc. SPIE **8461**, 846106 (2012).
[24] C. Kittel, Phys. Rev. **73**, 155 (1948).
[25] T. Schneider, A. A. Serga, T. Neumann, B. Hillebrands, and M. P. Kostylev, Phys. Rev. B **77**, 214411 (2008).